J Eng Math (2012) 72:107–124
DOI 10.1007/s10665-011-9466-4

Traveling waves along viscous filaments

A. C. T. Aarts · S. J. L. van Eijndhoven · O. Zavinska

Received: 18 December 2009 / Accepted: 21 March 2011 / Published online: 13 April 2011

Abstract In this article, deflections of a viscous filament in a classical fiber spinning set-up are analyzed. The deflections are considered in a direction perpendicular to the vertical equilibrium state of the spin line. The result is a traveling wave equation with non-uniform coefficients representing the non-uniform filament velocity and non-uniform tension in the spin line. Under neglect of air drag, the system is conservative with respect to an energy functional, so that its eigenmodes have purely imaginary characteristic values. A numerical analysis of the eigenmodes of the system reveals that deflections propagate from take-up wheel to spinneret, with frequencies being multiples of a basic frequency and amplitudes sinus shaped with the maximum being shifted toward the spinneret. From the numerical results, a formula is derived, which approximates the basic frequency and traveling wave velocity directly in terms of the spinning process parameters.

Keywords Deflection · Eigenmode · Fiber spinning · Frequency · Traveling wave · Viscous filament · Viscous string model

1 Introduction

In this article, we consider deflections in polymer spinning. In contrast to fluctuations in filament thickness, an instability referred to as draw-resonance, which has been investigated extensively in the literature (see for an overview, for instance, Petrie and Denn [20] and Larson [14]), we investigate deflections in a direction perpendicular to the spin line. We consider the classical fiber spinning set-up, in which the filament leaves the die of a spinneret with a fixed initial speed, and is drawn by a take-up wheel at the exit of the spinning device with a much larger fixed end speed. Since in an industrial process many filaments are spun close to each other, perturbations induced by vibrations may cause the spin line to deflect. As a result, the filaments may stick to each other which causes them to break; see Götz et al. [10].

The problem considered in this study concerns deflections of a viscous filament that moves between two fixed points; see Fig. 1. For an elastic string, with a uniform tension and string velocity, these deflections have been studied in detail by Archibald and Emslie [2] and by Swope and Ames [26]; a review of transverse vibrations of

A. C. T. Aarts (✉) · S. J. L. van Eijndhoven · O. Zavinska
Department of Mathematics and Computer Science, Technische Universiteit Eindhoven, P.O. Box 513, 5600 MB Eindhoven, The Netherlands
e-mail: a.c.t.aarts@tue.nl

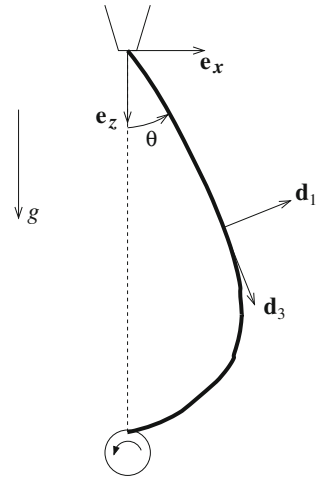

Fig. 1 The configuration of a filament in the $(\mathbf{e}_x, \mathbf{e}_z)$-plane, deflected from the vertical state in a classical spinning set-up

moving strings has been written by Chen [4]. In polymer spinning, however, the filament is drawn, so that the filament velocity, as well as the tension, is not uniform, but changes along the spin line.

To analyze deflections in polymer spinning, we need a constitutive equation that relates the filament velocity to the tension. Earlier articles reporting about the classical fiber spinning set-up assume a viscous fluid (i.e., Newtonian) model for the polymer, which has an elongational viscosity that is precisely three times the shear viscosity; cf. Matovich and Pearson [16]. In honor of Trouton [27], the elongational viscosity may be called the "Trouton viscosity." In general, a polymer exhibits viscoelastic behavior, which can be described by dedicated constitutive models, such as a Maxwell or Giesekus model. Because of its simplicity and effectiveness in capturing the basic characteristics of a polymer spinning process, however, in this article, we have adopted the viscous fluid model in terms of an elongational viscosity.

Many models to describe the flow of a thin viscous filament have been derived by various authors, e.g., Kase and Matsuo [12] and Pearson and Matovich [19] for uniaxial filaments, and Roos et al. [25] for curved filaments. These models determine the dynamics of the centerline based on cross-sectional averaging of the three-dimensional balance laws for mass and momentum. In the terminology of Antman [1], they are referred to as viscous "string" models; they do not describe the orientation of the cross section. The strict systematic asymptotic derivation from three-dimensional fluid dynamics has been carried out by, for instance, Dewynne et al. [7] and Cummings and Howell [6] for uniaxial filaments, and Panda et al. [18] and Marheineke and Wegener [15] for curved filaments. The models of Entov and Yarin [8], Yarin [30], Ribe [22], and Ribe et al. [23] also include the balance of angular momentum to describe the resistance against bending and twisting. In the sense of Antman [1], they are viscous Cosserat "rod" models; they also describe the orientation of the cross section. These models assume a moderately curved centerline and the filament sufficiently thin in comparison to the radius of curvature of the centerline. For instance, Ribe et al. [24] determine the stability of a viscous thread falling onto a horizontally moving belt to clarify the out-of-plane deflections observed by Chiu-Webster and Lister [5]. The reduction of a rod model to a string model for curved viscous filaments in which internal shearing forces are negligible has been derived by Arne et al. [3].

In this article, we use a two-dimensional viscous string model. For completeness of the article, we derive this model from the three-dimensional dynamical rod model of Ribe et al. [23], by neglecting the effects of resistance against bending and twisting. We describe the deflections of the filament in a classical spinning set-up, in which the equilibrium state of the filament is vertical; the deflections are perpendicular to the direction of spinning. We assume isothermal spinning conditions and neglect secondary effects such as surface tension and air drag. In Sect. 2, we introduce the full state of eight variables and describe the two-dimensional dynamics of the viscous filament, from which, the equilibrium state is derived, and subsequently, by linearization about that equilibrium state, a hyperbolic system for the deflections is determined, which satisfies a traveling wave equation. In Sect. 3, the mathematical model is analyzed, by identifying the analogy to a moving elastic string and determining an energy functional

of the system. The deflected state is characterized in terms of a phase, amplitude, and frequency of the eigenmodes of the system. Section 3.4 focuses on the equilibrium state for polymer spinning conditions, in terms of the Reynolds number and the draw ratio. In Sect. 4, numerical results are shown using the numerical method developed by Zavinska [31] to calculate the eigenvalues and eigenmodes of the hyperbolic system. These results quantify the amplitude, phase, and frequency for spinning conditions. Finally, guided by our numerical results, we arrive at a formula to determine the velocity at which the deflections travel along the spin line as well as their basic frequency, directly in terms of the spinning process parameters.

2 Mathematical model of a polymer filament in a classical spinning set-up

2.1 Two-dimensional viscous string model

We use a two-dimensional viscous string model, which we derive from the rod model introduced by Ribe et al. [23] by neglecting the effects of resistance against bending and twisting. The model describes the dynamics of the centerline of the polymer filament, based on the balance laws for mass and momentum. We neglect effects of surface tension and air drag.

We consider a filament with central axis in the $(\mathbf{e}_x, \mathbf{e}_z)$-plane, where the variables x (horizontal axis) and z (vertical axis) refer to a Cartesian coordinate frame with $\mathbf{e}_z$ pointing downward. Thus, the position of the central axis is described by $\mathbf{x}(s,t) = (x(s,t), 0, z(s,t))$, see Fig. 1, where arc length s and time t are the independent variables. The filament moves downward under the influence of a drawing force and gravity.

The tangent vector

$$\mathbf{t} = \frac{\partial x}{\partial s}\mathbf{e}_x + \frac{\partial z}{\partial s}\mathbf{e}_z$$

is a unit vector that defines the angle $\theta(s,t)$ according to

$$\frac{\partial x}{\partial s} = \sin\theta, \quad \frac{\partial z}{\partial s} = \cos\theta. \tag{1}$$

As in Ribe [22], we introduce the orthonormal moving reference frame $\{\mathbf{d}_1, \mathbf{d}_2, \mathbf{d}_3\}$, where $\mathbf{d}_3 = \mathbf{t}$, $\mathbf{d}_1 = \cos\theta\mathbf{e}_x - \sin\theta\mathbf{e}_z$, the normal to the tangent vector within the two-dimensional $(\mathbf{e}_x, \mathbf{e}_z)$-plane, and $\mathbf{d}_2 = \mathbf{e}_y$, with $\mathbf{e}_y$ the normal to that plane. The convective derivative D/Dt is defined by

$$\frac{D}{Dt} = \frac{\partial}{\partial t} + W\frac{\partial}{\partial s},$$

where W is the convective velocity. For slender filaments, the velocity W is regarded as the rate of change of the arc length parameter associated to a material point, that is, $W(\zeta(S,t),t) = \partial\zeta(S,t)/\partial t$, where the function ζ maps the material arc length parameter S to its position s according to $s = \zeta(S,t)$; see Marheineke and Wegener [15]. The velocity $\mathbf{U} = U_1\mathbf{d}_1 + U_3\mathbf{d}_3$ of the central axis satisfies

$$\begin{aligned} U_1 &= \cos\theta\,\tfrac{\partial x}{\partial t} - \sin\theta\,\tfrac{\partial z}{\partial t}, \\ U_3 &= W + \sin\theta\,\tfrac{\partial x}{\partial t} + \cos\theta\,\tfrac{\partial z}{\partial t}. \end{aligned} \tag{2}$$

The description of the filament kinematics is completed with the incompressibility condition:

$$\frac{\partial A}{\partial t} + \frac{\partial}{\partial s}(AW) = 0, \tag{3}$$

where A is the cross-sectional area, and where a constant and uniform mass density ρ is assumed.

The filament dynamics is governed by the balance of momentum equation:

$$\frac{\partial \mathbf{N}}{\partial s} + \rho A\mathbf{g} = \rho A\frac{D\mathbf{U}}{Dt}$$

with $\mathbf{g} = g\mathbf{e}_z$, the gravitational acceleration; and $\mathbf{N} = N_3\mathbf{d}_3$, the elongating force in the filament. Since

$$\frac{D}{Dt}(U_1\mathbf{d}_1) = \frac{DU_1}{Dt}\mathbf{d}_1 - U_1\frac{D\theta}{Dt}\mathbf{d}_3,$$
$$\frac{D}{Dt}(U_3\mathbf{d}_3) = \frac{DU_3}{Dt}\mathbf{d}_3 + U_3\frac{D\theta}{Dt}\mathbf{d}_1,$$

we get

$$\begin{aligned} N_3\tfrac{\partial\theta}{\partial s} - \rho g A\sin\theta &= \rho A\left(\tfrac{DU_1}{Dt} + U_3\tfrac{D\theta}{Dt}\right), \\ \tfrac{\partial N_3}{\partial s} + \rho g A\cos\theta &= \rho A\left(\tfrac{DU_3}{Dt} - U_1\tfrac{D\theta}{Dt}\right). \end{aligned} \tag{4}$$

Finally, we relate the elongating force to the velocity by the constitutive equation given by

$$N_3 = \eta_e A\frac{\partial W}{\partial s} \tag{5}$$

with η_e being the elongational viscosity. Equations 1–5 define a system of eight first-order partial differential equations for an eight-dimensional state vector $\mathbf{y} = (x, z, \theta, U_1, U_3, W, A, N_3)$.

The two-point boundary conditions that describe the filament under spinning conditions are

$$\begin{aligned} &x(0,t) = 0, \quad && z(0,t) = 0, \quad && U_1(0,t) = 0, \\ &W(0,t) = W_0, \quad && A(0,t) = A_0, \quad && x(L,t) = 0, \\ &z(L,t) = H, \quad && U_1(L,t) = 0, \quad && W(L,t) = Dr\,W_0, \end{aligned} \tag{6}$$

with H, being the spinning height, $A_0 = \pi R_0^2$ the initial cross-sectional area, R_0 the initial radius of the filament, W_0 the initial filament speed at the die exit, and Dr the draw ratio. The nine boundary conditions (6) thus determine the eight variables of state vector $\mathbf{y}$ and the unknown length $L = L(t)$ of the filament.

2.2 Equilibrium and deflected state

The equilibrium state $\mathbf{y}_{\text{eq}} = (x_{\text{eq}}, z_{\text{eq}}, \theta_{\text{eq}}, U_{1,\text{eq}}, U_{3,\text{eq}}, W_{\text{eq}}, A_{\text{eq}}, N_{3,\text{eq}})$ satisfies $L(t) = H, \theta_{\text{eq}} = 0$, $x_{\text{eq}} = 0, U_{1,\text{eq}} = 0, z_{\text{eq}} = z$, and $W_{\text{eq}} = U_{3,\text{eq}}$, while $(U_{3,\text{eq}}, A_{\text{eq}}, N_{3,\text{eq}})$ satisfies

$$\frac{\mathrm{d}}{\mathrm{d}z}(AU_3) = 0,$$
$$\frac{\mathrm{d}N_3}{\mathrm{d}z} + \rho g A = \rho A U_3\frac{\mathrm{d}U_3}{\mathrm{d}z},$$
$$N_3 = \eta_e A\frac{\mathrm{d}U_3}{\mathrm{d}z},$$

for $0 < z < H$. If gravity and inertia are neglected, than the equations are in correspondence with the differential equation derived by Kase and Matsuo [12]. Introducing the uniform mass flux $\Phi = \rho A U_3 = \rho A_0 W_0$, we write the three-dimensional system as

$$\begin{aligned} \frac{\mathrm{d}}{\mathrm{d}z}\left[\frac{N_3}{\Phi} - U_3\right] &= -\frac{g}{U_3}, \\ \frac{\mathrm{d}U_3}{\mathrm{d}z} &= \frac{\rho}{\eta_e\Phi}U_3N_3, \end{aligned} \tag{7}$$

with boundary conditions

$$U_3(0) = W_0, \quad U_3(H) = Dr\,W_0.$$

The tension $T = \eta_e \mathrm{d}U_3/\mathrm{d}z = N_3/A$ in the filament satisfies

$$T = \frac{\rho N_3 U_3}{\Phi}$$

where we use the relation for the uniform mass flux.

We linearize the system governed by Eqs. 1–5 about the equilibrium state $\mathbf{y}_{\text{eq}}(z) = \left(0, z, 0, 0, U_{3,\text{eq}}(z), U_{3,\text{eq}}(z), A_{\text{eq}}(z), N_{3,\text{eq}}(z)\right), 0 \le z \le H$, and consider the deflected state $\mathbf{y}_{\text{d}} = \mathbf{y}_{\text{d}}(z,t)$ in $\mathbf{e}_x$-direction of the form

$$\mathbf{y}_{\text{d}} = \left(x_{\text{d}}, 0, \theta_{\text{d}}, U_{1,\text{d}}, 0, 0, 0, 0\right).$$

The deflected state is determined by the system:

$$\frac{\partial x_{\text{d}}}{\partial z} = \theta_{\text{d}},$$

$$U_{1,\text{d}} = \frac{\partial x_{\text{d}}}{\partial t},$$

$$\left(N_{3,\text{eq}} - \rho A_{\text{eq}} U_{3,\text{eq}}^2\right)\frac{\partial \theta_{\text{d}}}{\partial z} - \rho g A_{\text{eq}}\theta_{\text{d}} = \rho A_{\text{eq}}\left[\frac{\partial U_{1,\text{d}}}{\partial t} + U_{3,\text{eq}}\frac{\partial U_{1,\text{d}}}{\partial z} + U_{3,\text{eq}}\frac{\partial \theta_{\text{d}}}{\partial t}\right],$$

with $0 < z < H$ and $t > 0$. Using the uniform mass flux, $\Phi = \rho A_{\text{eq}} U_{3,\text{eq}}$, we deduce from the system the second-order hyperbolic equation:

$$\left(N_{3,\text{eq}} - \Phi U_{3,\text{eq}}\right)\frac{\partial^2 x_{\text{d}}}{\partial z^2} - \frac{g\Phi}{U_{3,\text{eq}}}\frac{\partial x_{\text{d}}}{\partial z} = \frac{\Phi}{U_{3,\text{eq}}}\frac{\partial^2 x_{\text{d}}}{\partial t^2} + 2\Phi\frac{\partial^2 x_{\text{d}}}{\partial z \partial t}, \tag{8}$$

with boundary conditions

$$x_{\text{d}}(0,t) = 0, \quad x_{\text{d}}(H,t) = 0.$$

For polymer spinning conditions Φ, $U_{3,\text{eq}}$ and $N_{3,\text{eq}}$ are positive, with the viscous force generally much larger than the inertia force, so that $N_{3,\text{eq}} - \Phi U_{3,\text{eq}} > 0$. Equation 8 describes the deflected state of a spinning process where the constitutive behavior is embedded in the system via the elongational force $N_{3,\text{eq}}$ and the filament velocity $U_{3,\text{eq}}$. We used the Newtonian constitutive model to describe $N_{3,\text{eq}}$ and $U_{3,\text{eq}}$; of course, any other model such as a Giesekus or Maxwell model can replace the Newtonian model.

3 Analysis of the mathematical model

To analyze the deflections of the viscous filament in polymer spinning, we first identify, in Sect. 3.1, the analogy to a moving elastic string, whose governing equation and solution are put in Appendix A. In Sect. 3.2, we determine criteria for conservation and dissipation of energy of general hyperbolic systems, which we use in Sect. 3.3 to analyze the deflections in polymer spinning in terms of eigenmodes and characteristic values. Finally, in Sect. 3.4, we analyze the equilibrium state for polymer spinning conditions.

3.1 Analogy to a moving elastic string

In analogy to a moving elastic string (see Appendix A), for the viscous filament, we define the "classical" wave speed c in terms of the tension T_{eq} in the filament as

$$c(z)^2 = \frac{T_{\text{eq}}(z)}{\rho} = \frac{N_{3,\text{eq}}(z)\, U_{3,\text{eq}}(z)}{\Phi}$$

and the velocity c_{s} of the "string" itself, that is,

$$c_{\text{s}}(z) = U_{3,\text{eq}}(z).$$

Using the above velocities in Eq. 8, we obtain

$$\frac{\partial^2 x_{\text{d}}}{\partial t^2} + 2c_{\text{s}}(z)\frac{\partial^2 x_{\text{d}}}{\partial z \partial t} - \left(c(z)^2 - c_{\text{s}}(z)^2\right)\frac{\partial^2 x_{\text{d}}}{\partial z^2} + g\frac{\partial x_{\text{d}}}{\partial z} = 0. \tag{9}$$

Thus, comparing Eq. 9 to Eq. 28 within Appendix A, we see that the deflections of a moving viscous filament are governed by an equation equivalent to the one of an elastic string. The difference is that the tension, and thus the wave speed c, and the filament velocity c_s are not uniform along the spin line. In analogy to the velocity c_{tr} of a moving elastic string (see Eq. 31), for the viscous filament, we introduce

$$c_{tr}(z) = \frac{c(z)^2 - c_s(z)^2}{c_s(z)} = \frac{N_{3,eq}(z)}{\Phi} - U_{3,eq}(z).$$

Also c_{tr} is not uniform for a viscous filament.

The equilibrium state (7) written in terms of c_s and c_{tr} reads

$$\begin{aligned} \frac{dc_{tr}}{dz} &= -\frac{g}{c_s}, \\ \frac{dc_s}{dz} &= \frac{\rho}{\eta_e} c_s (c_{tr} + c_s). \end{aligned} \tag{10}$$

3.2 Conservation and dissipation of energy of hyperbolic systems

The moving elastic string and viscous filament in a classical fiber spinning set-up are examples of the following general hyperbolic second-order partial differential equation that we consider in this section:

$$\frac{\partial^2 w}{\partial z^2} = p(z) \frac{\partial^2 w}{\partial t^2} + 2q(z) \frac{\partial^2 w}{\partial z \partial t} + \alpha(z) \frac{\partial w}{\partial z} + \delta(z) \frac{\partial w}{\partial t} \tag{11}$$

for $0 < z < l$ and $t > 0$, subjected to the boundary conditions

$$w(0,t) = w(l,t) = 0, \quad t \geq 0.$$

We assume that $\alpha(z) \geq 0$, $\delta(z) \geq 0$. Introducing the variables u, v according to

$$u = \frac{\partial w}{\partial t}, \quad v = \frac{\partial w}{\partial z}$$

we get the first-order system:

$$\begin{aligned} \frac{\partial u}{\partial z} &= \frac{\partial v}{\partial t} \\ \frac{\partial v}{\partial z} &= p(z) \frac{\partial u}{\partial t} + 2q(z) \frac{\partial u}{\partial z} + \alpha(z) v + \delta(z) u \end{aligned} \tag{12}$$

with boundary conditions $u(0,t) = u(l,t) = 0$. From system (12), we derive

$$\frac{\partial}{\partial z}(uv) - \alpha(z) uv = \frac{1}{2} \frac{\partial}{\partial t} \left(p(z) u^2 + v^2 \right) + q(z) \frac{\partial}{\partial z} \left(u^2 \right) + \delta(z) u^2.$$

Let $r(z)$ be the integrating factor given by $\alpha(z) = r'(z)/r(z)$, i.e., $r(z) = \exp\left(\int_0^z \alpha(\zeta)\, d\zeta \right)$, then we obtain

$$\begin{aligned} \frac{1}{r(z)} u(z,t) v(z,t) = u(0,t) v(0,t) + \frac{1}{2} \frac{\partial}{\partial t} \int_0^z \frac{1}{r(\zeta)} \left(p(\zeta) u^2 + v^2 \right) d\zeta \\ + \int_0^z \frac{\delta(\zeta)}{r(\zeta)} u(\zeta)^2 d\zeta + \int_0^z \frac{q(\zeta)}{r(\zeta)} \frac{\partial}{\partial z} \left[u^2 \right] d\zeta. \end{aligned}$$

From the boundary conditions and partial integration, we derive

$$\int_0^l \frac{q(\zeta)}{r(\zeta)} \frac{\partial}{\partial z} \left[u^2 \right] d\zeta = - \int_0^l \frac{q'(\zeta) r(\zeta) - q(\zeta) r'(\zeta)}{r(\zeta)^2} u(\zeta)^2 d\zeta.$$

Thus, by defining the energy functional E of the system at time t as

$$E(u,v)|_t = \frac{1}{2}\int_0^l \frac{1}{r(\zeta)}\left(p(\zeta)u^2 + v^2\right)\mathrm{d}\zeta, \tag{13}$$

we obtain

$$\frac{\mathrm{d}E}{\mathrm{d}t} = -\int_0^l \frac{\delta(\zeta)r(\zeta) - q'(\zeta)r(\zeta) + q(\zeta)r'(\zeta)}{r(\zeta)^2}\,u(\zeta)^2\,\mathrm{d}\zeta.$$

We conclude that

– The system is dissipative with respect to the energy functional E if

$$\delta(z) > \tfrac{1}{r(z)}\left[q'(z)r(z) - \mathrm{d}(z)r'(z)\right], \quad \text{i.e.,} \quad \tfrac{\delta}{r} > \tfrac{\mathrm{d}}{\mathrm{d}z}\left[\tfrac{q}{r}\right],$$

or in terms of $\alpha(z)$

$$\delta(z) + \alpha(z)\,q(z) > q'(z). \tag{14}$$

– The systems is conservative with respect to the energy functional E if and only if

$$\frac{\delta}{r} = \frac{\mathrm{d}}{\mathrm{d}z}\left[\frac{q}{r}\right],$$

i.e.,

$$\delta(z) + \alpha(z)\,q(z) = q'(z). \tag{15}$$

3.3 Characteristics of the deflected state

Using the results of Sect. 3.2, we analyze the deflected state in polymer spinning by putting

$$w = x_\mathrm{d}, \quad u = U_{1,\mathrm{d}}, \quad v = \theta_\mathrm{d},$$

and

$$p(z) = \frac{1}{c_\mathrm{tr}(z)\,c_\mathrm{s}(z)}, \quad q(z) = \frac{1}{c_\mathrm{tr}(z)},$$
$$\alpha(z) = \frac{g}{c_\mathrm{tr}(z)c_\mathrm{s}(z)}, \quad \delta(z) = 0,$$

to write hyperbolic equation (9) in the form of (12):

$$\begin{aligned}\frac{\partial u}{\partial z} &= \frac{\partial v}{\partial t},\\ \frac{\partial v}{\partial z} &= \frac{1}{c_\mathrm{tr}(z)\,c_\mathrm{s}(z)}\frac{\partial u}{\partial t} + 2\frac{1}{c_\mathrm{tr}(z)}\frac{\partial v}{\partial t} + \frac{g}{c_\mathrm{tr}(z)\,c_\mathrm{s}(z)}v.\end{aligned} \tag{16}$$

Next, we define the eigenmodes, $\hat{u}$ and $\hat{v}$, and the characteristic values σ of hyperbolic system (16) by

$$u(z,t) = \hat{u}(z)\mathrm{e}^{\sigma t}, \quad v(z,t) = \hat{v}(z)\mathrm{e}^{\sigma t}.$$

They are determined from the characteristic equation:

$$\mathcal{B}_\mathrm{eq}\frac{d\hat{\mathbf{u}}}{dz} + \mathcal{C}_\mathrm{eq}\hat{\mathbf{u}} = \sigma\mathcal{A}_\mathrm{eq}\hat{\mathbf{u}}, \tag{17}$$

where $\hat{\mathbf{u}} = (\hat{u}, \hat{v})$, and

$$\mathcal{B}_\mathrm{eq} = \begin{pmatrix}1 & 0\\ 0 & 1\end{pmatrix}, \quad \mathcal{C}_\mathrm{eq} = \begin{pmatrix}0 & 0\\ 0 & \frac{g}{c_\mathrm{tr}c_\mathrm{s}}\end{pmatrix}, \quad \mathcal{A}_\mathrm{eq} = \begin{pmatrix}0 & 1\\ \frac{1}{c_\mathrm{tr}c_\mathrm{s}} & \frac{2}{c_\mathrm{tr}}\end{pmatrix}.$$

The characteristic equation is subject to the boundary conditions:

$$\hat{u}(0) = \hat{u}(H) = 0.$$

The complex eigenmodes can be written as

$$\hat{u}(z) = X_u(z)e^{i\varphi_u(z)}, \quad \hat{v}(z) = X_v(z)e^{i\varphi_v(z)},$$

where X_u, X_v are the amplitudes and φ_u, φ_v are the phases of u and v, respectively.

The energy functional E of system (16) at time t is equal to (cf. Eq. 13)

$$E(u,v)|_t = \frac{1}{2}\int_0^H \exp\left(-\int_0^z \frac{g}{c_{tr}(\zeta)c_s(\zeta)}d\zeta\right)\left[\frac{1}{c_{tr}(z)\,c_s(z)}u(z,t)^2 + v(z,t)^2\right]dz.$$

Using the equilibrium state equations (10), we see that the following relation holds:

$$q'(z) = -\left(\frac{1}{c_{tr}(z)}\right)^2 c'_{tr}(z) = -\left(\frac{1}{c_{tr}(z)}\right)^2\left(-\frac{g}{c_s(z)}\right) = \alpha(z)\,q(z).$$

Thus, with criteria (14)–(15) derived in Sect. 3.2, we conclude that the system described by (16) and (10) is conservative with respect to the functional E, so that $dE/dt = 0$. Thus, the characteristic values σ of this system are purely imaginary, and we put $\sigma = i\omega$, in which $\omega = 2\pi f$, with f being the frequency. The characteristic equation has a countable number of eigenfrequencies, f_n, to each of which a phase φ_n and amplitude X_n correspond, whence the deflections are determined by the functions:

$$X_n(z)\cos(\varphi_n(z) + 2\pi f_n t),$$

corresponding to waves traveling along the spin line. Since the characteristic values are purely imaginary, the waves are not damped.

3.4 Analysis of the equilibrium state

In this section, we analyze the equilibrium state in terms of c_s and c_{tr}, for polymer spinning conditions. In a dimension analysis, the equations are non-dimensionalized by scaling z by H, and the velocities by the initial velocity W_0 at the die exit. This results in two dimensionless numbers: the Reynolds number, $Re = \rho W_0 H/\eta_e$: the ratio of the inertia force and the viscous force, and the Froude number $Fr = W_0^2/(gH)$: the ratio of the inertia force and the gravitational force. Besides, we introduce $K = \sqrt{Re/Fr}$: the ratio of the gravitational force and the viscous force. In polymer spinning, typical values are $H = 10$ cm, $W_0 = 10$ cm/s, and $\rho = 1$ g/cm^3, while the elongational viscosity may well range from 1 to 16 kPa s. It means that both $Re \ll 1$ and $Fr \ll 1$, while K ranges from 0.25 to 1.

The dimensionless equilibrium-state equations (10) read

$$\begin{aligned}\frac{dc_{tr}}{dz} &= -\frac{1}{Fr}\left(\frac{1}{c_s}\right),\\ \frac{d}{dz}\left(\frac{1}{c_s}\right) &= -Re\left(1 + \frac{c_{tr}}{c_s}\right).\end{aligned} \tag{18}$$

By introducing the variables y_1 and y_2 according to

$$y_1 = (ReFr)^{\frac{1}{2}}c_{tr}, \quad y_2 = \frac{1}{c_s}$$

we transform system (18) into

$$\begin{aligned}\frac{dy_1}{dz} &= -Ky_2,\\ \frac{dy_2}{dz} &= -Re - Ky_1y_2,\end{aligned} \tag{19}$$

with boundary conditions $y_2(0) = 1$ and $y_2(1) = 1/Dr$. We approximate y_1 and y_2 by taking $Re = 0$ in the above equation. Thus, we obtain

$$\begin{aligned} &y_2 = 1 + \tfrac{1}{2}\left(y_1^2 - \gamma^2\right), \\ &\tfrac{\mathrm{d}y_1}{\mathrm{d}z} = -K\left(1 + \tfrac{1}{2}\left(y_1^2 - \gamma^2\right)\right), \\ &\gamma = y_1(0) \end{aligned} \tag{20}$$

If inertia forces are small compared to viscous forces (i.e., for $Re \ll 1$), the value of γ approximately equals $\sqrt{\eta_e/(g\rho W_0)}\,\mathrm{d}U_3/\mathrm{d}z|_{z=0}$, which in dimensionless form reads $\sqrt{Fr/Re}\,\mathrm{d}c_\mathrm{s}/\mathrm{d}z|_{z=0}$. Since in polymer spinning, viscous forces are large, we consider the case $\gamma^2 > 2$ and write $\gamma^2 = \beta^2 + 2$. The solution of (20) is given by

$$y_1(z;\beta) = \gamma\,\frac{1 + \frac{\beta}{\sqrt{\beta^2+2}}\tanh\left(\frac{1}{2}\beta K z\right)}{1 + \frac{\sqrt{\beta^2+2}}{\beta}\tanh\left(\frac{1}{2}\beta K z\right)},$$

$$y_2(z;\beta) = \frac{1}{\left(\cosh\left(\frac{1}{2}\beta K z\right) + \frac{\sqrt{\beta^2+2}}{\beta}\sinh\left(\frac{1}{2}\beta K z\right)\right)^2},$$

where β must be determined from the equation:

$$Dr = \Gamma(\beta) = \left(\cosh\left(\frac{1}{2}\beta K\right) + \frac{\sqrt{\beta^2+2}}{\beta}\sinh\left(\frac{1}{2}\beta K\right)\right)^2.$$

Typically, for $0 < \beta_1 < \beta_2$, we have

$$y_2(z;\beta_1) > y_2(z;\beta_2) \text{ for all } z, \quad 0 \le z \le 1,$$

and thus, in particular, $\Gamma(\beta_1) < \Gamma(\beta_2)$. Further,

$$y_2(z;\beta) > \lim_{\beta\downarrow 0} y_2(z;\beta) = \frac{1}{\left(1 + \frac{1}{2}\sqrt{2}Kz\right)^2},$$

and thus $\Gamma(\beta) > \left(1 + \frac{1}{2}\sqrt{2}K\right)^2$, i.e., only draw ratios larger than $\left(1 + \frac{1}{2}\sqrt{2}K\right)^2$ are feasible.

For K sufficiently small, a fair approximation of y_1 and y_2 is given by

$$y_1(z;\beta) = \sqrt{\beta^2+2} \quad \text{and} \quad y_2(z;\beta) = \exp(-z\log Dr),$$

where $\beta = (\log Dr)/K$. Thus, it follows that for $Re \ll Fr$ and $Dr > \left(1 + \sqrt{Re/(2Fr)}\right)^2$ the dimensional velocities are given by

$$\begin{aligned} &c_\mathrm{tr}(z) \cong \tfrac{W_0}{\sqrt{ReFr}}\sqrt{\tfrac{Fr}{Re}(\log Dr)^2 + 2} \cong \tfrac{W_0}{Re}\log Dr, \\ &c_\mathrm{s}(z) \cong W_0 \exp\left(\tfrac{z}{H}\log Dr\right). \end{aligned} \tag{21}$$

Relations (21) correspond to the equilibrium state under neglect of gravity and inertia, yielding a uniform elongating force $N_3 = \Phi(c_\mathrm{tr} + c_\mathrm{s}) \cong \Phi c_\mathrm{tr} \cong \eta_e A_0 W_0 \log(Dr)/H$; cf. Renardy [21]. Further, since $c_\mathrm{s} \ll c_\mathrm{tr}$ for Re sufficiently small, velocity c can be approximated by $c \cong \sqrt{c_\mathrm{s} c_\mathrm{tr}}$, implying that the tension is approximated by

$$T_\mathrm{eq}(z) \cong \rho W_0^2\,\frac{\log Dr}{Re}\exp\left(\frac{z}{H}\log Dr\right). \tag{22}$$

Finally, we note that the residence time t_eq of a fluid particle in the equilibrium state is given by (cf. Hyun [11])

$$t_\mathrm{eq} = \int_0^H \frac{\mathrm{d}z}{c_\mathrm{s}(z)} \cong \frac{H}{W_0\log Dr}\left(1 - \frac{1}{Dr}\right) \cong \frac{H}{W_0\log Dr}. \tag{23}$$

In the next section, we use results (21)–(23) of the equilibrium state for analyzing the numerically calculated deflections in polymer spinning.

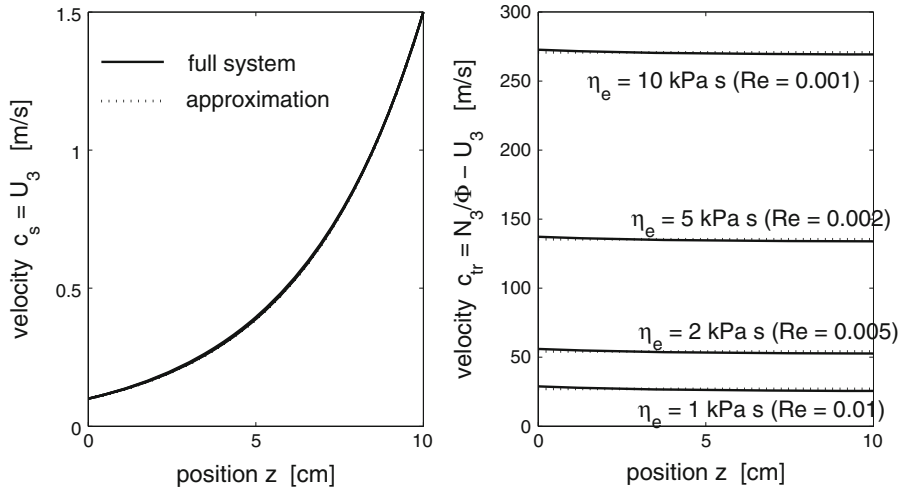

Fig. 2 The velocities $c_s(z)$ and $c_{tr}(z)$ of the equilibrium state of polymer spinning, obtained numerically from system (10) (*solid lines*) in comparison to the approximations given in (21) (*dotted lines*), for $Dr = 15$, $H = 10$ cm, and different viscosities η_e (so that $Fr = 0.01$ and Re varies, implying that K varies)

4 Results

In this section, we show the results for the deflections in polymer spinning. For the velocity W_0 at the die exit, we assume 10 cm/s, for the polymer mass density ρ, 1 g/cm^3, and for the diameter at the die exit $D_0 = 2R_0$, 1.5 mm.

We determine the equilibrium state, both numerically from the full system (10) and from the approximations (21) in which gravity and inertia have been neglected. In Figs. 2 and 3, the profiles of c_s and c_{tr} are shown. We observe that the equilibrium state is accurately described by the approximations (21). The difference between the approximations and the results of the full system is small, also for the relatively large value of $K = 1$ in case $Re = 0.01$. Thus, in polymer spinning, both inertia and gravity effects are small, so that the equilibrium-state velocity c_{tr} is almost uniform along the filament, implying that the viscous force N_3 is almost uniform along the filament. We see that the non-uniformity in c_{tr} is more pronounced at lower draw ratios and lower viscosity values. Furthermore, the equilibrium-state filament velocity profile $c_s = U_3$ is independent of viscosity; it depends only on the spinning height H, the draw ratio Dr, and the initial velocity W_0.

To determine the deflections in polymer spinning, we solve the characteristic equation (17) including its boundary conditions. The method to determine the solution is presented by Zavinska [31], who developed a numerical approach to calculate the characteristic values and eigenmodes of hyperbolic systems. The approach is based on a Galerkin method in which the eigenmodes are written as an expansion in terms of basis functions with unknown coefficients; the basis functions chosen are the so-called triangular functions. The numerical method has been used by Zavinska et al. [32] to determine the characteristics of draw resonance in polymer spinning. In Appendix A, the numerical method is validated for the moving elastic string (with uniform velocities). The results of the method for the deflections of a viscous filament will next be discussed.

In Fig. 4, the amplitudes X_n and phases φ_n for the deflection x_d in polymer spinning are shown for the first four eigenmodes, while in Table 1, the corresponding eigenfrequencies f_n are given for the first eight eigenmodes. We see that the frequency of each nth mode is almost equal to n times the frequency of the first mode, i.e., $f_n = n\, f_1$. Furthermore, the corresponding phases are linear as function of z, i.e., $\varphi_n(z) = z\Delta\varphi_n$, with $\Delta\varphi_n$ the (uniform) slope. As a result, the deflections travel with uniform velocity, $v_{tr,n} = 2\pi f_n/\Delta\varphi_n$, along the filament. Also, the slope of the phase of the nth mode is almost equal to n times the slope of the phase of the first mode, i.e., $\Delta\varphi_n = n\,\Delta\varphi_1$. Hence, the velocities $v_{tr,n}$ are almost equal to each other. By comparing the velocities $v_{tr,n}$ with approximation $(W_0/Re)\log(Dr) = 27.08$ m/s for the equilibrium-state velocity c_{tr} (see Eq. 21), we conclude that the traveling

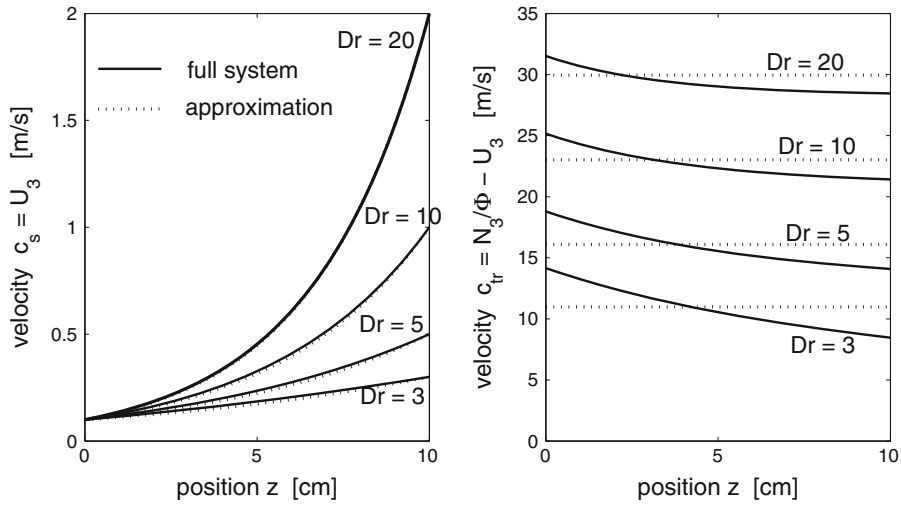

Fig. 3 The velocities $c_s(z)$ and $c_{tr}(z)$ of the equilibrium state of polymer spinning, obtained numerically from system (10) (*solid lines*) in comparison to the approximations given in (21) (*dotted lines*), for $\eta_e = 1$ kPa s, $H = 10$ cm, and different draw ratios Dr (so that $Fr = 0.01$ and $Re = 0.01$, implying that $K = 1$)

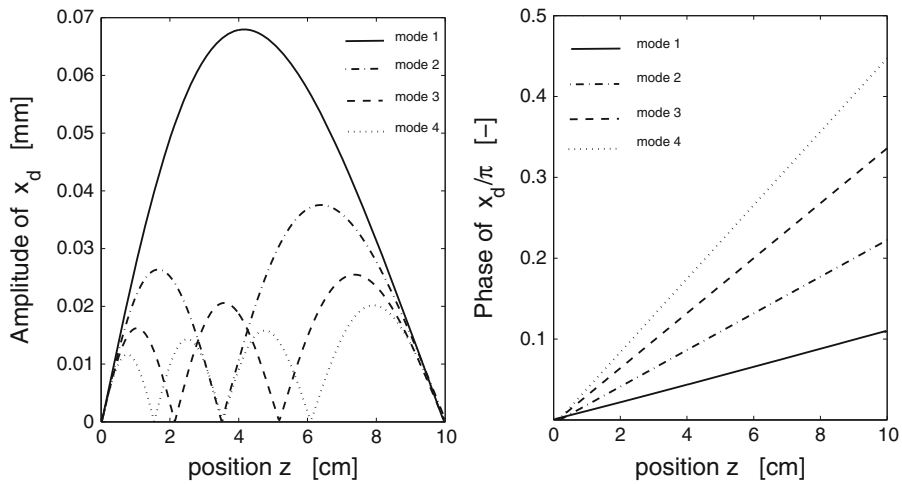

Fig. 4 The amplitude X_n (*left picture*) and phase φ_n (*right picture*) of the deflection x_d of polymer spinning for the first four eigenmodes, for $Dr = 15$, $H = 10$ cm, and $\eta_e = 1$ kPa s (so that $Re = 0.01$ and $Fr = 0.01$)

velocity $v_{tr,n}$ of each eigenmode of the deflections precisely corresponds to the equilibrium-state velocity c_{tr}. Since the phase is increasing as function of z (i.e., the slope $\Delta\varphi_n$ is positive), deflections propagate from the take-up wheel at $z = H$ toward the die exit of the spinneret at $z = 0$. This is in contrast to the waves in draw resonance, which have been found to travel in the opposite direction, i.e., from spinneret to take-up wheel, see Kim et al. [13]. Finally, we notice that the amplitude of the nth mode has $n + 1$ nodes and n antinodes. Here, the position of the antinode of the first mode, i.e., the position at which the amplitude reaches its maximum, is equal to $z_{an} = 0.416\,H$, indicating that the amplitudes are not a pure sinus, in contrast to the moving elastic string that has the position of the antinode of the first mode precisely at $z = H/2$; see Eq. 29.

Since the frequencies and traveling wave velocities of the deflections depend on the equilibrium state, we determine the basic frequency $f_{basic} = f_1\ (= f_n/n)$ and the traveling wave velocity $v_{tr} = v_{tr,1}\ (= v_{tr,n})$ for various draw ratios Dr and Reynolds numbers Re.

Table 1 The eigenfrequencies f_n, phase slopes $\Delta\varphi_n$, and traveling wave velocities $v_{\mathrm{tr},n}$ of the first eight eigenmodes for the deflections in polymer spinning, for $Dr = 15$, $H = 10$ cm, and $\eta_e = 1$ kPa s (so that $Re = 0.01$ and $Fr = 0.01$)

Mode n	f_n (Hz)	f_n/n (Hz)	$H\Delta\varphi_n/\pi$ (–)	$H\Delta\varphi_n/(n\pi)$ (–)	$v_{\mathrm{tr},n} = 2\pi f_n/\Delta\varphi_n$ (m/s)
1	14.81	14.81	0.1101	0.1101	26.91
2	29.83	14.92	0.2259	0.1130	26.41
3	44.83	14.94	0.3397	0.1132	26.39
4	59.82	14.96	0.4533	0.1133	26.39
5	74.79	14.96	0.5666	0.1133	26.40
6	89.78	14.96	0.6797	0.1133	26.42
7	104.74	14.96	0.7934	0.1133	26.40
8	119.72	14.97	0.9064	0.1133	26.42

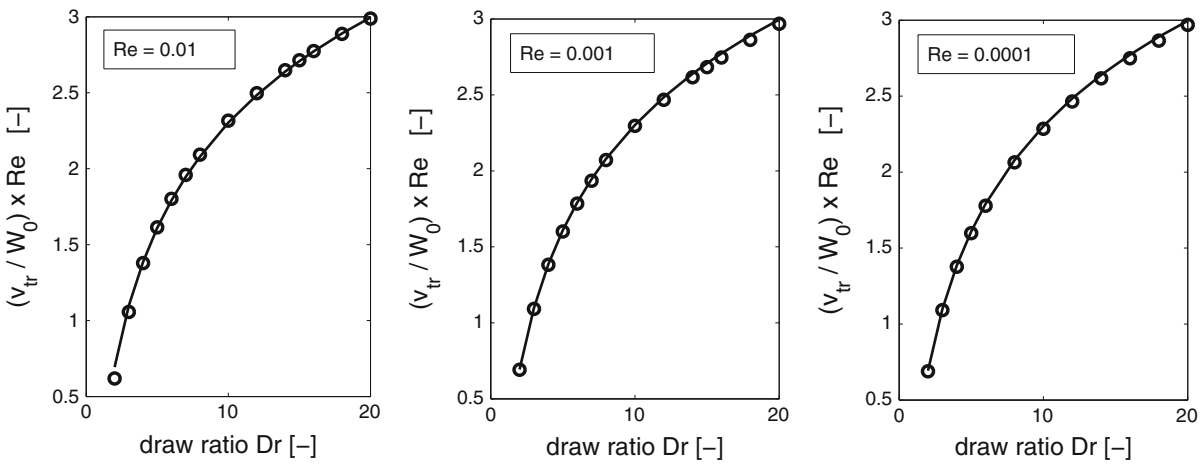

Fig. 5 The dimensionless traveling wave velocity $(v_{\mathrm{tr}}/W_0)Re$ for the deflections in polymer spinning (*symbols*) versus draw ratio Dr, in comparison to approximation (21) for the equilibrium-state velocity c_{tr} (*solid lines*), for $Fr = 0.01$ and different values of Re

In Fig. 5, the obtained traveling wave velocity is given versus draw ratio, for three different Reynolds numbers. We observe that v_{tr} increases with increasing draw ratio and that $(v_{\mathrm{tr}}/W_0)Re$ is independent of the Reynolds number, implying that $v_{\mathrm{tr}}/W_0 = G(Dr)/Re$ with G a function of the draw ratio only. We also compare v_{tr} to approximation (21) of the equilibrium-state velocity c_{tr}. From the excellent agreement shown in Fig. 5, we conclude that the traveling wave velocity v_{tr} of the deflections can be accurately determined from the equilibrium-state velocity $c_{\mathrm{tr}} \cong N_3/\Phi$, that is,

$$v_{\mathrm{tr}} \mathrel{\mathring{=}} c_{\mathrm{tr}} \cong \frac{W_0}{Re}\log Dr = \frac{\eta_e}{\rho H}\log Dr.$$

Thus, in polymer spinning the traveling wave velocity of deflections can be determined directly from the (uniform) elongating force and mass flux. As a result, it increases with increasing draw ratio and increasing viscosity, while it decreases with increasing spinning height and increasing mass density. Furthermore, it is independent of the initial velocity at the die exit.

The time t_{d} of the deflections to travel from take-up wheel to spinneret is equal to

$$t_{\mathrm{d}} = \frac{H}{v_{\mathrm{tr}}} = \frac{\rho H^2}{\eta_e \log Dr}.$$

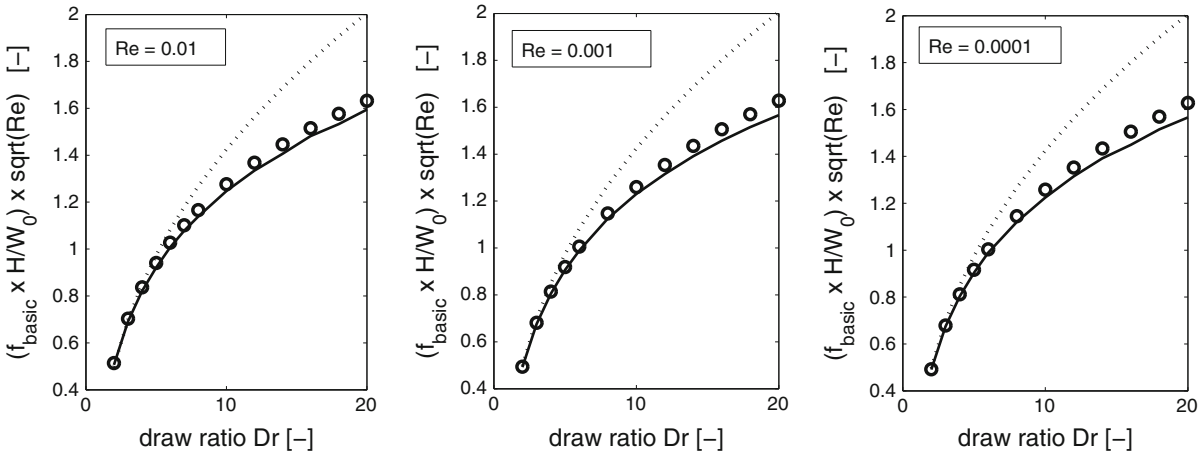

Fig. 6 The dimensionless basic frequency $(f_{\text{basic}} H/W_0)\sqrt{Re}$ for the deflections in polymer spinning (*symbols*) versus draw ratio Dr, in comparison to both approximation (25) based on the average tension (*dotted lines*) and approximation (26) based on the tension at antinode position z_{an} of the first mode (*solid lines*), for $Fr = 0.01$ and different values of Re

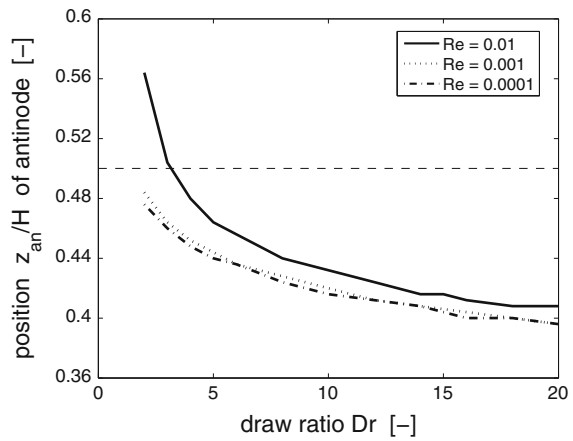

Fig. 7 The dimensionless position z_{an}/H of the antinode of the first mode for deflections in polymer spinning versus draw ratio Dr, for $Fr = 0.01$ and different values of Re

In comparison to the residence time t_{eq} of a particle in the equilibrium state, the travel time t_{d} of the deflections satisfies

$$\frac{t_{\text{d}}}{t_{\text{eq}}} = \frac{\rho H W_0}{\eta_e} = Re.$$

Since in polymer spinning $Re \ll 1$, the deflections thus move very fast so that they behave almost as standing waves.

In Fig. 6, the obtained basic frequency is given versus draw ratio, for three different Reynolds numbers. We observe that f_{basic} increases with increasing draw ratio, and that $(f_{\text{basic}} H/W_0)\sqrt{Re}$ is independent of the Reynolds number implying that it is a function of the draw ratio only. Thus, the basic frequency satisfies

$$f_{\text{basic}} = \frac{W_0}{H}\,\frac{1}{\sqrt{Re}}\,F(Dr),$$

with the function F to be determined. In contrast to the moving elastic string (see (32)), in polymer spinning, the basic frequency cannot be determined directly from the equilibrium state according to $f_{\text{basic}} = \left(c^2 - c_{\text{s}}^2\right)/(2Hc)$ since the velocities c and c_{s} depend on z. As a first approximation, we recognize that, for $Re \ll Fr$,

$$\frac{c^2 - c_{\text{s}}^2}{c} \cong c = \sqrt{\frac{T_{\text{eq}}}{\rho}}, \tag{24}$$

and subsequently we take the average value according to

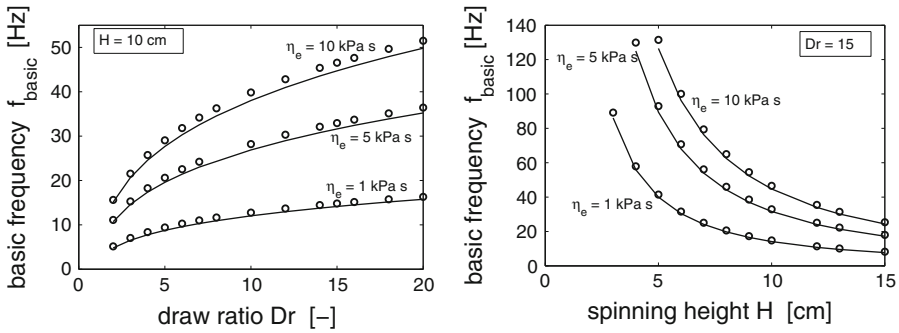

Fig. 8 The basic frequency f_{basic} for the deflections in polymer spinning (*symbols*), in comparison to the derived formula (27) (*solid lines*), for different values of η_e

$$\begin{aligned} f_{\text{basic}} &\stackrel{\circ}{=} \frac{1}{2H}\left[\frac{1}{H}\int_0^H \sqrt{\frac{T_{\text{eq}}(z)}{\rho}}\,\mathrm{d}z\right] \\ &\cong \frac{W_0}{H}\sqrt{\frac{\log Dr}{Re}}\left[\frac{1}{2H}\int_0^H \exp\left(\frac{z}{2H}\log Dr\right)\mathrm{d}z\right] \\ &= \frac{W_0}{H}\frac{\sqrt{Dr}-1}{\sqrt{\log Dr}}\frac{1}{\sqrt{Re}}, \end{aligned} \tag{25}$$

in which we used approximation (22) for the tension T_{eq}. In Fig. 6, we compare approximation (25) with the basic frequency obtained from the numerical calculations. We see that this approximation, obtained by averaging, overestimates the frequency, especially at larger draw ratios, and is not accurate enough. Using (24), we next approximate f_{basic} as

$$f_{\text{basic}} \stackrel{\circ}{=} \frac{1}{2H}\sqrt{\frac{T_{\text{eq}}(z_{\text{an}})}{\rho}} \cong \frac{W_0}{2H}\sqrt{\frac{\log Dr}{Re}}\exp\left(\frac{z_{\text{an}}}{2H}\log Dr\right) \tag{26}$$

to let the basic frequency be determined by the tension at the antinode position $z = z_{\text{an}}$ of the first mode, the position where the deflections have maximum amplitude. From the numerical calculations, we subsequently determine this antinode position. In Fig. 7, we show its dependence on draw ratio for three different Reynolds numbers. Using the obtained values in the above estimation, from Fig. 6, we conclude that the approximation given in (26) yields an accurate estimate for the basic frequency, indeed.

In Fig. 7, we also observe that the position of the antinode of the first mode hardly depends on the Reynolds number nor on the draw ratio. For large draw ratios and small Reynolds numbers, this position tends to the value $z_{\text{an}} = 0.4H$, implying that (see Eq. 26), in practice, the basic frequency can be approximated according to the following formula:

$$f_{\text{basic}} \cong \frac{W_0}{2H}\frac{1}{\sqrt{Re}}\,(\log Dr)^{0.7} = \frac{1}{2H}\sqrt{\frac{\eta_e W_0}{\rho H}}\,(\log Dr)^{0.7}\,. \tag{27}$$

The above equation indicates that the tension in the spin line that determines the basic frequency is equal to (cf. Eq. 22)

$$T(z_{\text{an}}) \cong \frac{\rho W_0^2}{Re}(\log Dr)^{1.4} = \frac{\eta_e W_0}{H}(\log Dr)^{1.4}.$$

In Fig. 8, the basic frequency, obtained from the numerical calculations, is plotted versus both draw ratio Dr and spinning height H, for different values of the elongating viscosity. From the comparison made with the derived formula (27), we conclude that the basic frequency of deflections in polymer spinning can be adequately determined from it. Thus, in polymer spinning, the basic frequency is related to the tension at the antinode position of the first mode. As a result, it increases with increasing draw ratio, with increasing viscosity, and with increasing initial speed, while it decreases with increasing spinning height and increasing mass density.

5 Conclusions

In this article, we have shown that deflections perpendicular to the spin line in a classical spinning set-up satisfy a traveling wave equation with non-uniform coefficients because of the non-uniform filament velocity and non-uniform tension in the spin line. Evaluation of this wave equation in terms of an energy functional revealed that (under neglect of air drag) the system has purely imaginary characteristic values. From numerical calculations, we found that the frequencies of the eigenmodes of these deflections are multiples of a basic frequency, and that the phases are multiples of the phase of the first mode, so that all eigenmodes have the same traveling velocity. Furthermore, we found that the traveling wave velocity relates directly to an equilibrium-state traveling velocity that is approximately equal to the (uniform) elongating force divided by the mass flux. The deflections are found to propagate from take-up wheel to spinneret, which is in opposite direction of the variations in filament thickness observed in draw resonance. Since inertia effects are small in polymer spinning, the deflections move very fast so that they behave almost as standing waves.

In contrast to a moving elastic string (with uniform velocity and tension), in polymer spinning, the basic frequency cannot be determined directly from the equilibrium state. From our numerical results, we found that the basic frequency is determined from the tension in the spin line at a position where the first mode of the deflections has a maximum amplitude. Guided by our numerical results, with the first mode having a maximum deflection at about 0.4 times the spinning height, we derived a formula to determine also the basic frequency explicitly in terms of the process parameters.

We note that, for spinning heights in the range of 5–10 cm, the basic frequency of deflections is large (in the order of 10–100 Hz) in comparison to the basic frequency obtained in draw resonance (which is in the order of 1 Hz, see, for instance, Pearson and Matovich [19], or Gelder [9]).

Appendix A: Moving elastic string

We analyze the deflections of a moving elastic string, whose equation has been derived first by Archibald and Emslie [2] and later by Swope and Ames [26]. For an elastic string that moves with positive uniform velocity c_s in the positive z-direction and has a uniform tension T_0, the equation for the deflection $w = w(z, t)$ from equilibrium is given by

$$\frac{\partial^2 w}{\partial t^2} + 2c_s \frac{\partial^2 w}{\partial z \partial t} - \left(c^2 - c_s^2\right) \frac{\partial^2 w}{\partial z^2} = 0, \tag{28}$$

where $c = \sqrt{T_0/\rho}$ represents the classical wave speed, with ρ the mass density; see Miranker [17]. In general, the tension in the string is so large that $c > c_s$. We assume boundary conditions to be $w(0, t) = w(l, t) = 0$.

The above equation is a reduced form of the general hyperbolic second-order partial differential equation (11) considered in Sect. 3.2 with $p(z) = p = 1/(c^2 - c_s^2)$, $q(z) = q = c_s/(c^2 - c_s^2)$, and $\delta(z) = \alpha(z) = 0$ (i.e., without air drag and without restoring force). Hence, the energy functional E of system (28) at time t is equal to (cf. Eq. 13)

$$E(u, v)|_t = \frac{1}{2} \int_0^l \left[\frac{1}{c^2 - c_s^2} u\,(z, t)^2 + v\,(z, t)^2 \right] \mathrm{d}z,$$

where $u = \partial w/\partial t$ and $v = \partial w/\partial z$, and it satisfies $\mathrm{d}E/\mathrm{d}t = 0$. Note that this functional is not the sum of the kinetic and potential energies; cf. Wickert and Mote Jr. [28].

With the use of the variables u and v, we obtain the system:

$$\frac{\partial u}{\partial z} = \frac{\partial v}{\partial t},$$
$$\frac{\partial v}{\partial z} = \left(a^2 - b^2\right) \frac{\partial u}{\partial t} + 2b \frac{\partial v}{\partial t},$$

Table 2 The eigenfrequencies f_n, phase slopes $\Delta\varphi_n$, and traveling wave velocities $v_{\mathrm{tr},n}$ of the first eight eigenmodes for the deflections of the moving elastic string, for $l = 10$ cm, $c_\mathrm{s} = 0.517$ m/s, and $c = 3.777$ m/s (so that $c_\mathrm{tr} = 27.08$ m/s, $f_\mathrm{basic} = 18.532$ Hz, and $l\Delta\varphi_n/(n\pi) = 0.1369$ according to (30)–(32))

Mode n	f_n (Hz)	f_n/n (Hz)	$l\Delta\varphi_n/\pi$ (–)	$l\Delta\varphi_n/(n\pi)$ (–)	$v_{\mathrm{tr},n} = 2\pi f_n/\Delta\varphi_n$ (m/s)
1	18.531	18.531	0.1373	0.1373	26.99
2	37.067	18.533	0.2737	0.1368	27.09
3	55.593	18.531	0.4117	0.1372	27.01
4	74.132	18.533	0.5476	0.1369	27.07
5	92.658	18.532	0.6858	0.1372	27.02
6	111.195	18.533	0.8219	0.1370	27.06
7	129.725	18.532	0.9594	0.1371	27.04
8	148.257	18.532	1.0966	0.1371	27.04

with a, b being defined by

$$c = \frac{a}{a^2 - b^2}, \quad c_\mathrm{s} = \frac{b}{a^2 - b^2},$$

i.e.,

$$a = \frac{c}{c^2 - c_\mathrm{s}^2}, \quad b = \frac{c_\mathrm{s}}{c^2 - c_\mathrm{s}^2},$$

so that $0 \le b < a$. The system is subjected to the boundary conditions $u(0, t) = u(l, t) = 0$.

We determine eigenmodes, $\hat{u}_n$, $\hat{v}_n$, and characteristic values, ω_n, by writing

$$u(z, t) = \hat{u}_n(z)\, \mathrm{e}^{\mathrm{i}\omega_n t}, \quad v(z, t) = \hat{v}_n(z)\, \mathrm{e}^{\mathrm{i}\omega_n t},$$

and find from straightforward calculations that

$$\omega_n = \pm\frac{n\pi}{al}, \quad n = 1, 2, \ldots$$

and

$$\begin{pmatrix} \hat{u}_{\pm n} \\ \hat{v}_{\pm n} \end{pmatrix}(z) = \mathrm{e}^{\pm\frac{n\pi bz}{al}\mathrm{i}} \begin{pmatrix} \sin\left(\frac{n\pi z}{l}\right) \\ b\sin\left(\frac{n\pi z}{l}\right) \mp ia\cos\left(\frac{n\pi z}{l}\right) \end{pmatrix},$$

in correspondence to the solution obtained by Wickert and Mote Jr. [29] by means of Green's function method. We focus on the first component of the nth eigenmode $\hat{u}_n$ that can be expressed as

$$\hat{u}_n(z) = X_n(z)\, \mathrm{e}^{\mathrm{i}\varphi_n(z)}$$

where $X_n(z)$ is its amplitude and $\varphi_n(z)$ its phase given by

$$X_n(z) = \left|\sin\left(\frac{n\pi z}{l}\right)\right| \tag{29}$$

and

$$\varphi_n(z) = \frac{n\pi b}{al} z + \left[\frac{nz}{l}\right]\pi. \tag{30}$$

Here $[\cdot]$ denotes the floor function such that $[\alpha + n] = n$ for $\alpha \in [0, 1)$.

Assume $b \neq 0$. In combination with the time factor $\mathrm{e}^{\mathrm{i}\omega_n t}$, the modes $\hat{u}_n$ and $\hat{u}_{-n}$ determine the waves

$$\cos\left(\frac{n\pi b}{al}(z + c_\mathrm{tr} t)\right)\sin\left(\frac{n\pi z}{l}\right), \quad \sin\left(\frac{n\pi b}{al}(z + c_\mathrm{tr} t)\right)\sin\left(\frac{n\pi z}{l}\right)$$

that are traveling with velocity

$$c_{\mathrm{tr}} = \frac{1}{b} = \frac{c^2 - c_{\mathrm{s}}^2}{c_{\mathrm{s}}} \tag{31}$$

from $z = l$ to $z = 0$ if $b > 0$, and from $z = 0$ to $z = l$ if $b < 0$; nodes are in the points $z_{n,k} = (k/n)l,\ k = 0, \ldots, n$. The basic frequency is given by

$$f_{\mathrm{basic}} = \frac{1}{2al} = \frac{c^2 - c_{\mathrm{s}}^2}{c}\,\frac{1}{2l}. \tag{32}$$

Note that if $b = 0$, i.e., $c_{\mathrm{s}} = 0$ and $c = 1/a$, we obtain the known standing waves

$$\cos\left(\frac{n\pi}{al}t\right)\sin\left(\frac{n\pi z}{l}\right), \quad \sin\left(\frac{n\pi}{al}t\right)\sin\left(\frac{n\pi z}{l}\right).$$

We validate the numerical approach of Zavinska [31] by calculating the characteristic values and eigenmodes of the moving elastic string equation (28) using this approach, and comparing them to the exact solutions given in (29)–(32). In Table 2, the eigenfrequencies f_n are given for the first eight eigenmodes. We see that indeed each frequency f_n of the nth mode is (almost) equal to n times the frequency f_1 of the first mode, with f_n/n in excellent agreement with the value $f_{\mathrm{basic}} = 18.532$ Hz according to (32). Furthermore, we found that (not shown here) the phase φ_n is linear as function of z, i.e., $\varphi_n(z) = z\Delta\varphi_n$, in correspondence with (30). Also, each slope $\Delta\varphi_n$ of the phase of the nth mode is indeed almost equal to n times the phase slope $\Delta\varphi_1$ of the first mode, with $l\Delta\varphi_n/(n\pi)$ in good agreement with the value $l\Delta\varphi_n/(n\pi) = c_{\mathrm{s}}/c = 0.1369$ according to (30). As a result, the obtained value $v_{\mathrm{tr},n}$ is in good correspondence with the value $c_{\mathrm{tr}} = 27.08$ m/s of (31). Thus, the numerical approach is adequate to determine the eigenvalues and eigenmodes of a hyperbolic system such as the moving elastic string.

References

1. Antman SS (2005) Nonlinear problems of elasticity. Springer, New York
2. Archibald FR, Emslie AG (1958) The vibration of a string having a uniform motion along its length. ASME J Appl Mech 25(3): 347–348
3. Arne W, Marheineke N, Wegener R (2010) Asymptotic transition from Cosserat rod to string models for curved viscous inertial jets. Technical report Fraunhofer Institut Techno- und Wirtschaftsmathematik, No. 192
4. Chen LQ (2005) Analysis and control of transverse vibrations of axially moving strings. ASME Appl Mech Rev 58:91–115
5. Chiu-Webster S, Lister JR (2006) The fall of a viscous thread onto a moving surface: a 'fluid-mechanical sewing machine'. J Fluid Mech 569:89–111
6. Cummings LJ, Howell PD (1999) On the evolution of non-axisymmetric viscous fibres with surface tension, inertia and gravity. J Fluid Mech 389:361–389
7. Dewynne JN, Ockendon JR, Wilmott P (1992) A systematic derivation of the leading-order equations for extensional flows in slender geometries. J Fluid Mech 244:323–338
8. Entov VM, Yarin AL (1984) The dynamics of thin liquid jets in air. J Fluid Mech 140:91–111
9. Gelder D (1971) The stability of fiber drawing processes. Ind Eng Chem Fundam 10(3):534–535
10. Götz T, Rave H, Reinel-Bitzer D, Steiner K, Tiemeier H (2001) Simulation of the fiber spinning process. Technical report Fraunhofer Institut Techno- und Wirtschaftsmathematik, No. 26
11. Hyun JC (1978) Theory of draw resonance: I Newtonian fluids. AICh E J 24:418–422
12. Kase S, Matsuo T (1965) Studies on melt spinning. I. Fundamental equations on the dynamics of melt spinning. J Polym Sci A 3:2541–2554
13. Kim BM, Hyun JC, Oh JS, Lee SJ (1996) Kinematic waves in the isothermal melt spinning of Newtonian fluids. AIChE J 42: 3164–3169
14. Larson RG (1992) Instabilities in viscoelastic flows. Rheol Acta 31:213
15. Marheineke N, Wegener R (2009) Asymptotic model for the dynamics of curved viscous fibres with surface tension. J Fluid Mech 622:345–369
16. Matovich MA, Pearson JRA (1969) Spinning a molten threadline. Steady-state isothermal viscous flows. Ind Eng Chem Fundam 8:512–520

17. Miranker WL (1960) The wave equation in a medium in motion. IBM J 4(1):36–42
18. Panda S, Marheineke N, Wegener R (2008) Systematic derivation of an asymptotic model for the dynamics of curved viscous fibres. Math Methods Appl Sci 31:1153–1173
19. Pearson JRA, Matovich MA (1969) Spinning a molten threadline. Stability. Ind Eng Chem Fundam 8:605–609
20. Petrie CJS, Denn MM (1976) Instabilities in polymer processing. AIChE J 22:209
21. Renardy M (2006) Draw resonance revisited. SIAM J Appl Math 66(4):1261–1269
22. Ribe NM (2004) Coiling of viscous jets. Proc Roy Soc Lond A 460:3223–3239
23. Ribe NM, Habibi M, Bonn D (2006a) Stability of liquid rope coiling. Phys Fluids 18(8):84102-1–84102-12
24. Ribe NM, Lister JR, Chiu-Webster S (2006b) Stability of a dragged viscous thread: onset of "stitching" in a fluid-mechanical "sewing machine". Phys Fluids 18(12):124105-1–124105-8
25. Roos JP, Schweigman C, Timman R (1973) Mathematical formulation of the laws of conservation of mass and energy and the equation of motion for a moving thread. J Eng Math 7(2):139–146
26. Swope RD, Ames WF (1963) Vibrations of a moving threadline. J Frankl Inst 275(1):36–55
27. Trouton FT (1906) On the coefficient of viscous traction and its relation to that of viscosity. Proc Roy Soc A 77:426–440
28. Wickert JA, Mote CD Jr (1989) On the energetics of axially moving continua. J Acoust Soc Am 85(3):1365–1368
29. Wickert JA, Mote CD Jr (1990) Classical vibration analysis of axially moving continua. ASME J Appl Mech 57(3):738–744
30. Yarin AL (1993) Free liquid jets and films hydrodynamics and rheology. Longman, Harlow
31. Zavinska O (2008) Spectral analysis of polymer elongation processes. PhD thesis, Technische Universiteit Eindhoven
32. Zavinska O, Claracq J, van Eijndhoven SJL (2008) Non-isothermal film casting: determination of draw resonance. J Non-Newton Fluid Mech 151(3):21–29